Characterizing brain connectivity using ϵ-radial nodes: application to autism classification

Nagesh Adluru*, Moo K. Chung, Kim M. Dalton
Andrew L. Alexander, and Richard J. Davidson

University of Wisconsin, Madison, WI, USA

Abstract. Whole brain tractography studies of can generate up to and over half-a-million tracts per brain which form the basis for constructing edges in an extremely large $3D$ graph. Currently there is no agreed-upon method for constructing the brain anatomical connectivity graphs out of large number of white matter tracts. In this paper, we present an efficient framework for building and analyzing graphs using tractography in a normalized space. We then apply the constructed graphs in a classification setting of autistic vs. typically developing individuals and obtain prediction accuracy of 87%. This suggests that efficiently characterizing anatomical connectivities of the brain may be used to characterize discriminant patterns in different populations.

1 Introduction

White matter which forms the basis of structural connectivity has been shown to be abnormal for example in regions like corpus callosum, in various autism studies [1, 2]. Characterizing global anatomical connectivity will significantly impact the study of brain pathology and such developmental disorders [3]. There is a growing interest of mapping out anatomical connectivity at a macroscale *in vivo* with the advancement of various Diffusion MRI acquisition techniques. A graph is a mathematical representation of a real-world complex system and is defined by a collection of nodes (vertices) and edges (links) between pairs of nodes. The nature of nodes and links in individual brain networks may be determined by combinations of brain mapping methods, anatomical parcellation schemes, and measures of connectivity. The nature of nodes and edges largely determines the neurobiological interpretation of network topology [4, 5].

Streamline tractography is typically used to characterize structural connectivity between two regions (nodes) in the brain. Here we propose that streamlines can be used to construct the nodes as well. Currently there is no agreed-upon method for constructing brain connectivity graphs out of a large number of white matter tracts. In this paper, we present an efficient, scalable and automated framework for building and analyzing ϵ-radial anatomical connectivity matrices (ϵ-acms) in a normalized space. Automatically identifying nodes using

* Contact author: adluru@wisc.edu. The authors are with Waisman Laboratory for Brain Imaging and Behavior at University of Wisconsin, Madison, WI, USA.

tract data has several advantages: (1) Cross-modality registration, which can have limitations when acquisition parameters vary, can be avoided. (2) Large scale studies become feasible with automated methods.

By using state-of-the-art spatial normalization ([6]) and tractography tools ([7]) the ϵ-acms show promising discriminative power in the context of classifying autism. The source code in MATLAB implementation is available on an accompanying website[1].

2 Related Work

Improved methods for mapping anatomical connectivity is an important step in exploring causal relationships in functional correlations [8, 9]. Fonteijn et. al. [10] attempt at providing anatomical basis for functional networks but they point out the problem of normalization of tracts and that there is no agreed-upon way of transferring anatomical landmarks into subject space without affecting tractography. Gong et. al. [11] applied DTI to map a network of anatomical connections between 78 cortical regions. Hagmann et. al. [12] constructed a connection matrix from fiber densities measured between homogeneously distributed and equal-sized regions of interest (ROIs) numbering between 500 and 4000. They identify ROIs by a heuristical two-phase "region growing" of voxels in the white/grey matter boundary. They show results on only two human subjects where they find that their individual brain networks have an exponential node degree distribution and that their global organization is in the form of a small world. Skudlarski et. al. [9] present an approach in which they use tractography to first estimate the strength of anatomical connection for any two white matter voxels and then using the neighboring white matter voxels they extend the connectivity information between pairs of grey matter voxels by using the information from neighboring white matter voxels. They perform tractography in the native space and use only up to 40000 tracts on average per subject. Further they use B0 images for non-linear registration for performing statistical analyses which does not guarantee that the underlying fiber architecture (defined by FA or $\lambda 1$) is in register [13].

In addition to using state-of-the-art tensor based normalization scheme, our framework is scalable up to a million tracts and we perform graph based classification on a dataset of 31 subjects. Fig. 1 shows the overview of the construction and analyses of ϵ-radial anatomical connectivity matrices (ϵ-acms). The next section describes the details of our ϵ-radial node and edge construction algorithms followed by experimental results and conclusions.

3 ϵ-radial anatomical connectivity

In this section we describe how to construct an anatomical connectivity matrix using streamlines without parcellations of the grey or white matter. The method uses the end points of the tracts to define the nodes by clustering neighboring

[1] http://brainimaging.waisman.wisc.edu/∼adluru/ERG/eacm.htm

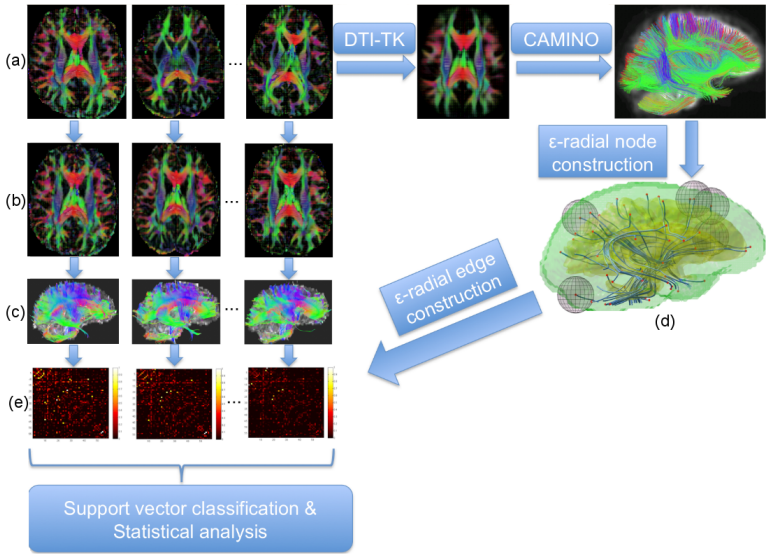

Fig. 1. (a) The input tensor volumes are used to generate a population specific atlas using DTI-TK. Tractography is performed on the atlas volume. (b) The individual subjects are transformed into the normalized space. (c) Tractography is performed on the individual volumes in the normalized space. (d) ϵ-radial nodes are constructed using Alg. 1. (e) ϵ-acms are constructed using Alg. 2, which can be used for classification and other statistical analyses.

tract end points into a set of spheres of ϵ radius. These spheres form the nodes for constructing a connectivity matrix. We call the resulting connectivity as ϵ-radial connectivity. Using tract endpoint clusters as nodes allows to focus on regions where there is structural connectivity. The nodes although sphere shaped can be useful in localizing important regions of the brain. These ϵ-radial nodes are typically near the grey matter/white matter interface (useful to study connectivities between functional areas [12]) where the FA drops below 0.15, the tractography stopping criterion. The lower the stopping threshold, the more nodes will be in grey matter.

The following two algorithms describe how to identify the ϵ-radial nodes ($\mathcal{N}$) and edges efficiently. We would like to note that the connectivity matrices are currently built using the presence of *end points* in these spheres but can be extended to "passing through/way point" connectivity. Sample tracts connecting two different pairs of nodes, a set of ϵ-radial nodes and sample ϵ-radial anatomical connectivity are shown in Fig. 2.

Time complexity: If there are n tracts, the construction of kd-tree and ϵ-radial nodes takes $O(n \log^2 n)$. The construction of the ϵ-acm (with N nodes) takes $O(N \log^2 N + n \log^2 N)$ time. Most connectivity matrix algorithms estimate connectivity between nodes pairwise and are not scalable in the number of nodes and tracts as $O(nN^2) >> O(N \log^2 N + n \log^2 N)$. The proposed algorithm can

Algorithm 1 Construction of ϵ-radial nodes ($\mathcal{N}$)

Input: Set of n tracts in population specific atlas
$\mathcal{N} \leftarrow \Phi$ (empty set)
Build a kd-tree ($\mathcal{K}_{\mathcal{P}}$) on the end points, $\mathcal{P} = \{p_i\}_{i=1}^{2n}$ of the tracts
repeat
  Pick an element $p_k \in \mathcal{P}$
  $\mathcal{N} \leftarrow \mathcal{N} \cup \{p_k\}$
  $\mathcal{P} \leftarrow \mathcal{P} - \{p_j\}$ (set minus), where $\{p_j\}$ in ϵ-radius of p_k using $\mathcal{K}_{\mathcal{P}}$
until $\mathcal{P} = \Phi$
Output: $\mathcal{N}$

Algorithm 2 Construction of ϵ-radial anatomical connectivity matrix (ϵ-acm)

Input: Set of tracts, $\{t_i\}_{i=1}^{n}$ of the input volume in the normalized space and $\mathcal{N}$
Build a kd-tree ($\mathcal{K}_{\mathcal{N}}$) on the ϵ-radial nodes, $\mathcal{N}$
Initialize the square matrix ϵ-acm$[N][N]$ to zeros, where $N = |\mathcal{N}|$
for $i = 1$ to n **do**
  $n_1 \leftarrow$ node indices in ϵ radius of the first end point of t_i using $\mathcal{K}_{\mathcal{N}}$
  $n_2 \leftarrow$ node indices in ϵ radius of the second end point of t_i using $\mathcal{K}_{\mathcal{N}}$
  $n_1 \leftarrow n_1 - n_2$ (set minus)
  ϵ-acm$[n_1, n_2] \leftarrow \epsilon$-acm$[n_1, n_2] + 1$
end for
ϵ-acm $\leftarrow \epsilon$-acm $+ \epsilon$-acm^T (transpose)
Output: ϵ-acm

scale up to a million tracts very easily as the connectivity matrix is populated in *one pass* through the tracts. Connectivity matrices using about 200000 tracts take less than a minute on a typical machine and in MATLAB implementation.

Different resolutions of ϵ produce different sets of nodes and connectivity matrices. Sample ϵ-acms for a subject at different resolutions can be seen in Fig 3. As $\epsilon \rightarrow 0$, $N \rightarrow 2n$ where each tract end point becomes an ϵ-radial node and the connectivity matrix becomes very sparse and has unit entries. Using very large sparse connectivity matrices for any reasonable statistical analysis is very hard with the small sizes of datasets used in various studies. For the experiments presented we chose $\epsilon = 8mm$, which produced 58 nodes. We used $\epsilon = 8mm$ following the heuristics of Fonteijn et. al. [10], where they state "In most of the original studies [15-19,22], the ROIs that were used for effective connectivity analysis were all spheres of 8mm radius." in Sec. 2.3.

Alg. 1 is dependent on the order of points $p_k \in \mathcal{P}$. Our initial experiments suggest that although there is slight variance in spatial locations of the nodes, some global properties like histograms of node-degrees and edge-weights are stable. There seem to be some interesting connections between ϵ-acms and approximate neighborhood graphs used in simplical complexes ([14]) which need further exploration. Simplical complexes extract topological representations underlying point cloud data. In our case the tract end points form the point cloud data.

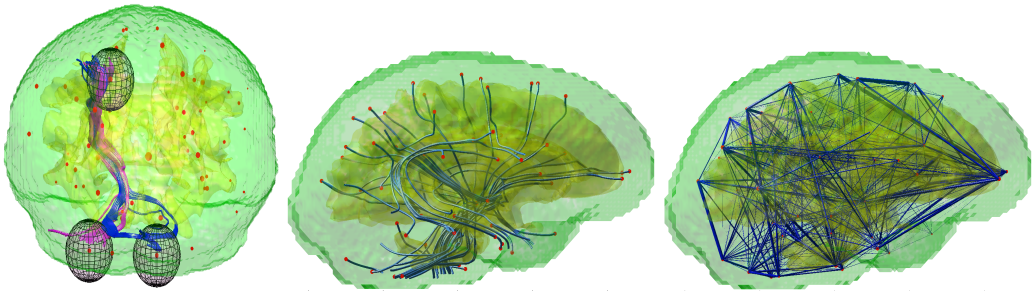

(a) (b) (c)

Fig. 2. Tracts whose end points are within the ϵ-radial spheres characterize the edges. (a) Tracts between two pairs of nodes are shown in different color. Size of the nodes is proportional to the degree of the nodes. (b) ϵ-radial node locations (red) on the template volume with the tracts that are responsible in identifying them. The nodes and tracts are overlaid on white matter (yellow) and grey matter (green). (c) Connectivities of the ϵ-radial nodes are shown using edges. The thickness of an edge is proportional to the number of tracts connecting two nodes.

4 Experimental results

Pre-processing and spatial normalization: DTI data from 31 subjects were used: 17 subjects with autism spectrum disorders (ASD) and 14 control subjects matched for age, handedness, IQ, and head size. The diffusion weighted images were acquired in 12 non-collinear diffusion encoding directions with diffusion weighting factor of $b = 1000s/mm^2$ in addition to a single ($b = 0$) reference image. Eddy current related distortion and head motion of each data set were corrected using AIR [15] and distortions from field inhomogeneities were corrected using field maps. The tensor elements were calculated using non-linear estimation using CAMINO [7].

Spatial normalization of diffusion tensor images plays a key role in constructing brain network graphs with identical nodes in the template. The quality of spatial normalization determines the extent to which white matter tracts are aligned. It has direct impact on the successful removal of shape confounds and consequently on the validity, specificity, and sensitivity of the subsequent statistical inferences of group differences. State-of-the-art diffusion tensor image registration DTI-TK [6] was used for spatial normalization of the subjects. Tensor volumes, with axial dimension equal to a power of 2, are better suited for registration algorithms that require the construction of standard multi-resolution image pyramids. Hence the tensor volumes were resampled to a voxel space of $128 \times 128 \times 64$ with voxel dimensions equal to 1.5mm $\times$ 1.75mm $\times$ 2.25mm. Streamline tractography based on TENsor Deflection (TEND, implemented in CAMINO [7]) was then used to generate the fiber tracts in the individual subjects transformed to the normalized space. The summary of the pre-processing can also be seen in Fig. 1.

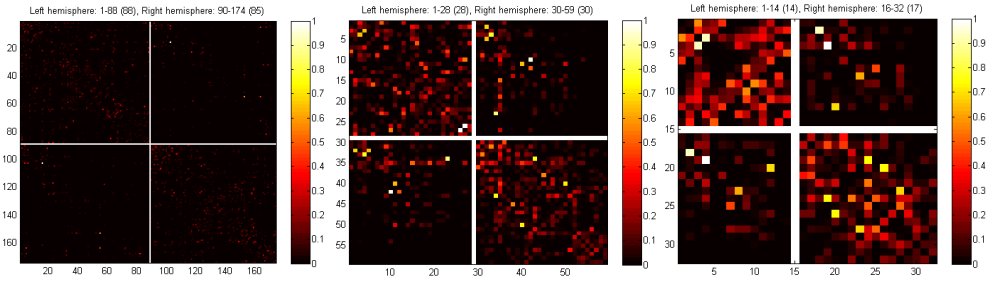

(a) (b) (c)

Fig. 3. ϵ-anatomical connectivity matrices (acms) of a sample subject at different resolutions of ϵ. (a) $\epsilon = 5mm$, $N = 173$ (b) $\epsilon = 8mm$, $N = 58$ (c) $\epsilon = 10mm$, $N = 31$. As ϵ decreases the number of nodes increases and the connectivity matrix becomes sparser. The ϵ-acms are normalized as $\epsilon\text{-acm} \leftarrow \frac{\epsilon\text{-acm} - \min(\epsilon\text{-acm})}{\max(\epsilon\text{-acm}) - \min(\epsilon\text{-acm})}$. The bright lines separate the hemispheric connectivities.

Support vector classification: The ϵ-radial nodes were identified in the population specific template as described in Alg. 1. Then for each of the individual subjects in the normalized space, ϵ-radial anatomical connectivity is obtained using Alg. 2. We filtered out tracts having fewer than 50 points to avoid the influence of spurious tracts. On average there were about 92000 tracts in each subject and the average longest tract had about 1500 points. On average the graph construction per subject takes about 18 seconds including file I/O on a 64-bit machine and using MATLAB implementation. Based on our survey of the existing tools for connectivity construction ours is the fastest automatic method. We explored two feature vectors viz. degree of nodes and weights of edges, for the classification experiments. Degree of nodes is simply calculated by summing up the rows or columns of adjacency matrices. The node-degree feature vector is N long while the edge-weight feature vector is $\frac{N(N-1)}{2}$ long. We use the popular support vector machines [16] with radial basis kernel as a classifier.

Since we have only 31 examples we evaluate our classifier performance using leave-one-out cross-validation scheme. For each fold we perform feature selection using simple t-tests (only on training data) and keep features that have p-values below a certain threshold. When using edge weight distributions as feature vectors, the average accuracy over 31 folds is 87% with 84% specificity and 94% sensitivity. When using degree of nodes the results are 84% accuracy, 83% specificity and 88% sensitivity. The classifier output values and the corresponding receiver operating characteristic (ROC) curves are shown in Fig. 4[2]. The average areas under curve (AUC) for the two features are 0.912 and 0.811 respectively.

Although edge weight distribution has higher cross-validation accuracy, there are more samples that fall inside the margin which could imply that degree

[2] One of the TD samples (subject 11 of the 14) in (c) although correctly classified, is not shown because the corresponding output made the figure out of scale.

of nodes is more generalizable feature. Increased discriminative power of edge-weights could be attributed to the "pair-wise" interactions while increased generalizability of node-degrees to lower dimensionality of the feature vector. Further exploration on sensitivity to ϵ, different feature extractions (e.g. hemispheric connectivities) and combinations (e.g. multi-kernel setting) is part of our future work.

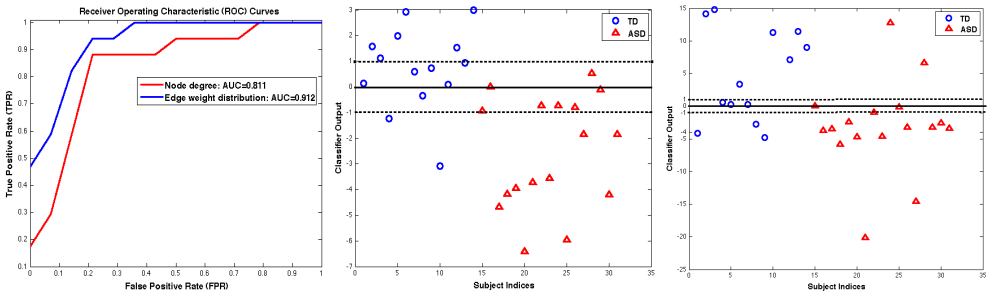

(a) (b) (c)

Fig. 4. (a) ROC curve shows for the two features. Edge weight distribution (blue) performs better than degree of nodes (red). (b,c) Classifier output values for the two classes. The thick line is the classification boundary and the dotted lines are the margins. Values above the thick line are classified as controls and those below as individuals with ASD. Blue circles represent Typically Developing (TD) individuals and the red triangles represent individuals diagnosed with Autism Spectrum Disorder (ASD). Edge weight distribution (b) has more examples in the margin compared to that using node degrees (c).

5 Discussion and conclusions

In this paper we proposed an automated and efficient way to build and analyze anatomical connectivities of brains. Our method of connectivity matrix construction could be applied to cases where the nodes are manually identified as well. The ϵ-radial connectivity method revealed significant group differences between ASD and controls and is consistent with current hypotheses of abnormal brain connectivity in autism [3, 17, 18]. Ideally, connectome maps acquired through the use of diffusion imaging should be cross-validated with anatomical data collected by histological techniques.

Acknowledgments

We thank Jee Eun Lee for eddy current correcting and field map correcting the DWI volumes. This work was partially supported by NIH grants MH62015, MH084051, MH080826 and CIBM-MIR fellowship.

References

1. Alexander, A., Lee, J., Lazar, M., et. al.: Diffusion tensor imaging of the corpus callosum in autism. Neuroimage **34**(1) (2007) 61–73

2. Pardini, M., Garaci, F., Bonzano, L., et. al.: White matter reduced streamline coherence in young men with autism and mental retardation. Eur. J. Neurol **16**(11) (2009) 1185–1190
3. Just, M., Cherkassky, V., Keller, T., et. al.: Functional and anatomical cortical underconnectivity in autism: Evidence from an fMRI study of an executive function task and corpus callosum morphometry. Cerebral Cortex **17** (2007) 951–961
4. Butts, C.: Revisiting the foundations of network analysis. Science **325** (2009) 414–416
5. Zalesky, A., Fornito, A., Harding, I., et. al.: Whole-brain anatomical networks: Does the choice of nodes matter? Neuroimage **50**(3) (April 2010) 970–983
6. Zhang, H., Yushkevich, P., Alexander, D., Gee, J.: Deformable registration of diffusion tensor MR images with explicit orientation optimization. **10** (2006) 764–785
7. Cook, P., Bai, Y., Nedjati-Gilani, S., et. al.: Camino: Open-source Diffusion-MRI reconstruction and processing. In: ISMRM. (2006) 2759
8. Sporns, O., Tononi, G., Kotter, R.: The human connectome: A structural description of the human brain. PLOS Computational Biology **1**(4) (2005)
9. Skudlarski, P., Jagannathan, K., Calhoun, V., et. al.: Measuring brain connectivity: diffusion tensor imaging validates resting state temporal correlations. Neuroimage **43**(3) (2008) 554–561
10. Fonteijn, H., Norris, D., Verstraten, F.: Exploring the anatomical basis of effective connectivity models with DTI-based fiber tractography. Journal of Biomedical Imaging **2008**(3) (2008) 1–9
11. Gong, G., He, Y., Concha, L., et. al.: Mapping anatomical connectivity patterns of human cerebral cortex using in vivo diffusion tensor imaging tractography. Cereb Cortex **19**(3) (2009) 524–536
12. Hagmann, P., Kurant, M., Gigandet, X., et. al.: Mapping human whole-brain structural networks with Diffusion MRI. PLoS one **2**(7) (2007)
13. Alexander, A., Lobaugh, N. In: Insights into Brain Connectivity Using Quantitative MRI Measures of White Matter. Springer Berlin (2007) 221–273
14. Zomorodian, A.: Fast construction of the Vietoris-Rips complex. Computer and Graphics **34**(3) (June 2010) 263–271
15. Woods, R., Grafton, S., Holmes, C., et. al.: Automated image registration: I. general methods and intrasubject, intramodality validation. Journal of Computer Assisted Tomography **22** (1998) 139–152
16. Chang, C., Lin, C.: LIBSVM: a library for support vector machines. (2001) Software available at `http://www.csie.ntu.edu.tw/~cjlin/libsvm`.
17. Kana, R., Keller, T., Minshew, N., Just, M.: Inhibitory control in high functioning autism: Decreased activation and underconnectivity in inhibition networks. Biological Psychiatry **62** (2007) 198–206
18. Sahyoun, C., Belliveau, J., Souliéres, I., et. al.: Neuroimaging of the functional and structural networks underlying visuospatial vs. linguistic reasoning in high-functioning autism. Neuropsychologia **48**(1) (2010) 86–95